

**UNA COMPARACIÓN DE REDUCCIÓN DE RUIDO EN IMÁGENES
DIGITALES UTILIZANDO UN MODELADO ESTADÍSTICO DE
COEFICIENTES WAVELET Y FILTRADO DE WIENER**

**A COMPARISON OF DIGITAL IMAGE DENOISING USING STATISTICAL
MODELING OF WAVELET COEFFICIENTS AND WIENER FILTERING**

**PhD. Francisco García-Ugalde*, PhD. Karina Pérez-Daniel*, MEng. Laura Reyes
Ruíz*, PhD. Manuel Cedillo-Hernández**, PhD. Antonio Cedillo-Hernández**, PhD.
Mariko Nakano-Miyatake**, PhD. Héctor Pérez-Meana****

* **Universidad Nacional Autónoma de México**, Facultad de Ingeniería, División de
Ingeniería Eléctrica, Departamento de Procesamiento de Señales.
Ciudad Universitaria, 04510 Ciudad de México, México.
Teléfono (+52)(55)56223011, E-mail: fgarciau@unam.mx

** **Instituto Politécnico Nacional**, SEPI-Escuela Superior de Ingeniería Mecánica y
Eléctrica Culhuacán.
Ave. Santa Ana 1000, San Francisco Culhuacán, Ciudad de México, México.
Teléfono (+52)(55)57296000 extensión 73256, E-mail: mcedillohdz@hotmail.com

Resumen: Este trabajo presenta un método de disminución de ruido en imágenes digitales, basado en un enfoque Bayesiano de dos etapas con ajuste empírico. Se estiman los coeficientes de una transformada wavelet de la imagen donde se ha reducido el ruido, utilizando una estimación lineal con un criterio de minimización del error cuadrático medio. Estos coeficientes constituyen una estimación deseable de la varianza de los coeficientes wavelet de la imagen libre de ruido.

Palabras clave: Disminución de ruido en imágenes digitales, Transformada wavelet, Filtrado de *Wiener*.

Abstract: This paper presents an image denoising method based on a two-step empirical Bayes approach. A linear minimum mean squared error-like estimation is performed to estimate the wavelet coefficients of the denoised image. These coefficients rely on a suitable estimation of the variance of the wavelet coefficients for the “clean” image.

Keywords: Digital image denoising, Wavelet transform, *Wiener* filtering.

1. INTRODUCTION

The quality of the noise reduction in images relies on the goodness of the models involved. This is particularly true when dealing with real world images. Though image denoising and image compression are two different fields, one can take advantage of some known models primarily defined in the context of image compression and reoriented them through image denoising. These

models recognize the existence of significant spatial dependencies using data structures such as zerotrees (Shapiro, 1993). The *Embedded Zerotree Wavelet* (EZW) algorithm generates a binary chain progressively ordered based on the relative importance of bits (embedded chain). This technique takes advantage of the existing correlation between wavelet coefficients of different subbands. Thus, given a coefficient $c[k_1/2, k_2/2]_{j+1}$, irrelevant in magnitude at scale $j+1$, it is

highly probable that the coefficient $c[k_1, k_2]_j$ at scale j is also irrelevant. In this way, coefficients conveying the most information are given a higher priority during compression. In the EZW algorithm a coefficient is irrelevant when it is lower than a predetermined threshold T . This translates analytically into the conditional probability:

$$P\left(c[k_1, k_2]_j \leq T \mid c\left[\frac{k_1}{2}, \frac{k_2}{2}\right]_{j+1} \leq T\right) \approx 1 \quad (1)$$

Thus, the EZW algorithm after wavelet transforming the image and with (1), represent the image coefficients by a tree structure where each root corresponds to a *father* wavelet coefficient $c[k_1/2, k_2/2]_{j+1}$ and its four *descendant* branches $c[k_1, k_2]_j$, as illustrated in Fig. 1.

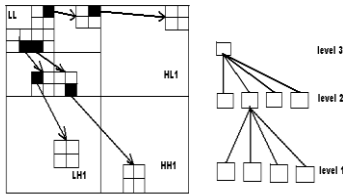


Fig. 1. The relations between wavelet coefficients in different subbands and associated tree structure.

The analysis must verify that no *descendant* element can be analyzed before its *father*. This restriction ensures that in the multiresolution structure associated, the low frequency subbands are being completely scanned before the higher ones can be processed. The scan order starts with the lowest frequency band LL_N , it continues to HL_N , LH_N , HH_N , then the coefficients at level $N-1$ are considered, and so on. Thus, we can deduce that the high performance of the zerotree-based image coders leads to the development of similar methods for image denoising. In (Chang *et al.*, 2000; Arivazhagan *et al.*, 2011) an image adaptive model was used to perform image denoising via wavelet thresholding using context modeling of the *global* coefficient histogram. A different approach has been proposed in (Mihcak *et al.*, 1999a) which exploits the *local* structure of wavelet image coefficients. As a different approach, in this paper a mixed criterion is considered: a local structure of wavelet image coefficients is exploited to estimate the variance of the wavelet coefficient of a “clean” image. This estimation is performed *only in positions* corresponding to *father* and *descendant* coefficients greater than an empirically established threshold T .

2. STATISTICAL MODELING OF WAVELET COEFFICIENTS

Many compression algorithms are based on the *Discrete Wavelet Transform* (DWT) as it concentrates most information in very few coefficients. Moreover, as explained in the previous section, the relationship between coefficients of different subbands can be exploited. Wavelet coefficients within subbands can be modeled as independent identically distributed (i.i.d.) random variables with a generalized *Gaussian* distribution (Mallat, 1989). This characteristic is the base of many compression and noise reduction algorithms. More sophisticated and perhaps less complex algorithms can be reached when considering the spatial interdependence between coefficients. In noise reduction problem, it has been observed that better results can be achieved when considering spatial interrelation or adaptability between coefficients. This is particularly true with real world images.

2.1. Minimum mean squared error estimator for the “clean” image

In each scale, the wavelet coefficients show a behavior based on a zero mean *Gaussian* distribution. Considering that the wavelet transform used is orthogonal, then the DWT of a noisy image $g[x_1, x_2]$, corrupted with an additive white *Gaussian* noise, can be described in the wavelet domain by,

$$c_g[k_1, k_2] = c_f[k_1, k_2] + c_n[k_1, k_2] \quad (2)$$

Where c_g , c_f and c_n are, respectively, the wavelet coefficients of the noisy image $g[x_1, x_2]$, the coefficients of the noiseless or “clean” image $f[x_1, x_2]$, and the coefficients of the noise image $n[x_1, x_2]$. Since the addition of two independent *Gaussian* random variables generates another *Gaussian* random variable with variance equal to the sum of the variances:

$$\sigma_{c_g}^2 = \sigma_{c_f}^2 + \sigma_{c_n}^2 \quad (3)$$

As $\sigma_{c_g}^2$ can be evaluated and assuming that $\sigma_{c_n}^2$ can be estimated (see section 3), then $\sigma_{c_f}^2$ is obtained by:

$$\begin{aligned}\sigma_{c_f}^2 &= \sigma_{c_g}^2 - \sigma_{c_n}^2 \\ &= \frac{1}{MN} \left(\sum_{k_1=1}^M \sum_{k_2=1}^N (c_g[k_1, k_2] - \mu_{c_g})^2 \right) - \sigma_{c_n}^2 \quad (4) \\ &= \frac{1}{MN} \sum_{k_1=1}^M \sum_{k_2=1}^N c_g^2[k_1, k_2] - \sigma_{c_n}^2\end{aligned}$$

Applying the minimum mean-squared error estimation theory to the wavelet coefficients of the noisy image, it is possible to obtain an approximation of each coefficient \hat{c}_f using the following equation.

$$\hat{c}_f[k_1, k_2] = \frac{\sigma_{c_f}^2}{\sigma_{c_f}^2 + \sigma_{c_n}^2} c_g[k_1, k_2] \quad (5)$$

It should be noted that (4) uses the entire wavelet domain resulting in lost in local information leading to poor value of the variance of the wavelet coefficient for f and subsequently poor estimates of its wavelet coefficients. Hence, to overcome the limitations introduced by (4), the proposed approach uses equation (5) where the maximum likelihood criterium estimates $\hat{\sigma}_{c_f}^2$, of the underlying variance field, and then are substituted for $\sigma_{c_f}^2$.

2.2. Maximum likelihood estimator for the underlying variance field $\hat{\sigma}_{c_f}^2$

New models for image wavelet coefficients has been introduced in (Mihcak *et al.*, 1999a; Arivazhagan *et al.*, 2011), inspired by a compression method previously published in (Lo Presto *et al.*, 1997). These models assume the existence of an unknown smooth space-variant variance field. Under these assumptions the wavelet coefficients can be modeled as independent random variables locally identically distributed. This suggests a high correlation between variances of adjacent coefficients. Considering a square neighborhood window $W_{m \times m}$ centered at coefficient $c_g[k_1, k_2]$, the variance can be written as

$$\sigma_{c_g}^2(k_1, k_2) \approx \sigma_{c_g}^2(k_1 + i, k_2 + j), i, j = -\frac{m-1}{2}, \dots, -1, 0, 1, \dots, \frac{m-1}{2} \quad (6)$$

where the neighborhood dimension m is a small odd integer number so that $c_g[k_1, k_2]$ is at the center of the window and the locally i.i.d.

assumption holds. Under the assumption of a variance field, a maximum likelihood estimator can be applied to compute the local variances of the coefficients of f . Based on (4) the ML variance estimator for the “clean” image using the neighborhood window $W_{m \times m}$ is given by,

$$\hat{\sigma}_{c_f}^2(k_1, k_2) \approx \max \left(0, \frac{1}{m^2} \sum_{i, j = -\frac{m-1}{2}}^{\frac{m-1}{2}} c_g^2[k_1 + i, k_2 + j] - \sigma_{c_n}^2 \right) \quad (7)$$

The choice of equation (7) over more sophisticated solutions (Mihcak *et al.*, 1999b; Jaiswal and Upadhyay, 2015) results from experimental observations. Experiments conducted with more accurate but more computationally demanding estimators for $\hat{\sigma}_{c_f}^2(k_1, k_2)$ and $\sigma_{c_n}^2$ have shown to have little effect on the noise reduction process. Hence, the proposed simpler solution (7) is retained.

3. ESTIMATION OF THE VARIANCE OF THE NOISY WAVELET COEFFICIENTS

The literature usually assumes that the variance of the noise wavelet coefficients $\sigma_{c_n}^2$ is an unknown parameter. However in practice it can be estimated, and it has been proven for a noise image $n(x_1, x_2)$ that its corresponding wavelet coefficients $c_n(k_1, k_2)$ possess a zero mean *Gaussian* distribution, thus maintaining the validity of the developments presented in previous sections.

Moreover in many applications, the variance of the wavelet coefficients of the noise image $n(x_1, x_2)$ within the finest scale is very close to that of the noisy image $g(x_1, x_2)$ at the same scale. Hence, a good estimate value for $\sigma_{c_n}^2$ can be found from:

$$\sigma_{c_n}^2 \approx \sigma_{c_g}^2 \quad \text{at scale } j = 1 \quad (8)$$

Thus, the estimation considers only coefficients at the first level of the decomposition, in subbands LH_1 , HL_1 and HH_1 .

4. ALGORITHM INTEGRATION

The noise reduction algorithm proposed in this paper firstly decompose the image into pyramid subbands at different scales; secondly denoise each

subband, except for the lowpass residual band and finally invert the pyramid transform. More details are summarized below:

- (i) A discrete wavelet transform is developed with L levels. Considering that $L=2$ is sufficient to distinguish noisy coefficients from important information, experimentations have been conducted with biorthogonal wavelets, symlets, coiflets and Daubechies's wavelets. However, only the most representative results achieved with the *coiflet5* wavelet are presented here.
- (ii) A zero matrix D_j for each subband in each scale is defined. Dimensions of this matrix must be the same as the corresponding subband.
- (iii) The wavelet coefficients of the approximation band are compared with an empirically chosen threshold T .
- (iv) Estimate the variance $\hat{\sigma}_{c_f}^2$ for only the *fathers* and *descendants* coefficients greater than T . An appropriate value for the threshold T must be chosen depending on the noise level and the wavelet used in the decomposition. Each estimated variance is associated to the corresponding element of matrix D_j . Thus, the matrix D_j contains all the necessary $\hat{\sigma}_{c_f}^2$ values for the computation of the wavelet coefficients \hat{c}_f in step (v).
- (v) With equation (5), the wavelet coefficients are computed for the denoised image and subsequently used to reconstruct the denoised image by the inverse DWT.

5. RESULTS

Experimentation with reference images is necessary to evaluate the performance of the algorithm. Four different images f , frequently used in the literature *Lena*, *Barbara*, *Woman Dark-Hair* and *Woman Blonde* have been used in this work. Our experiments are carried out on a personal computer running Microsoft Windows 10 OS© 64 bits with an Intel© Core i5-6600 processor (@3.3 GHz) and 16 GB RAM memory while the denoising procedure was implemented on Matlab© version R2016b. A noise image is simulated with *Gaussian* noise, zero mean and variance σ_n , and added to the original image to produce the noisy image g .

Figures 2, 6, 10 and 14 display the original images. The noisy images with *Gaussian* noise, zero mean and standard deviation $\sigma_n = 10$, in a scale from 0 to 255, are displayed in Figures 3, 7, 11 and 15. Comparative results of *Lena*, *Barbara*, *Woman Dark-Hair* and *Woman Blonde* are presented in Tables I, II, III and IV respectively. The image visual quality distortion is measured using the following well known indices (Jaiswal *et al.*, 2014): Peak Signal to Noise Ratio (PSNR), Structural Similarity Index (SSIM) (Wang *et al.*, 2004) and Quality Index Based on Local Variance (QILV) (Aja *et al.*, 2006).

Also for comparison purposes the denoising *Wiener* function of Matlab© is used. Our method (OM) is tested with three different window sizes: OM[3x3], OM[5x5] and OM[7x7]; different noise standard deviation and the *coiflet5* wavelet in the decomposition with a threshold $T=0.07$. Figures 4 and 5 provide a visual comparison of *Lena*, Figures 8 and 9 of *Barbara*, Figures 12 and 13 of *Woman Dark-Hair* as well as Figures 16 and 17 of *Woman Blonde*.

Table I. *Lena*

	$\sigma_n = 10$	$\sigma_n = 15$	$\sigma_n = 20$
	PSNR (dB)	PSNR (dB)	PSNR (dB)
WITHOUT FILTER	28.18	24.67	22.17
WIENER	33.6	31.18	29.04
OM[3x3]	34.09	31.54	29.46
OM[5x5]	34.4	32.11	30.3
OM[7x7]	34.42	32.21	30.5
	MSSIM	MSSIM	MSSIM
WITHOUT FILTER	0.6151	0.4523	0.3444
WIENER	0.8611	0.7856	0.6941
OM[3x3]	0.8733	0.7973	0.7156
OM[5x5]	0.8851	0.8284	0.7634
OM[7x7]	0.8861	0.8337	0.778
	QILV	QILV	QILV
WITHOUT FILTER	0.7738	0.5047	0.2996
WIENER	0.952	0.947	0.9107
OM[3x3]	0.9712	0.9496	0.9153
OM[5x5]	0.9596	0.939	0.9145
OM[7x7]	0.9559	0.93	0.8995

Table II. Barbara

	$\sigma_n = 10$	$\sigma_n = 15$	$\sigma_n = 20$
	PSNR (dB)	PSNR (dB)	PSNR (dB)
WITHOUT FILTER	28.16	24.66	22.2
WIENER	29.89	28.34	26.9
OM[3x3]	31.68	30.1	28.54
OM[5x5]	31.52	30.01	28.63
OM[7x7]	31.29	29.85	28.55
	MSSIM	MSSIM	MSSIM
WITHOUT FILTER	0.7154	0.5792	0.4793
WIENER	0.8501	0.7969	0.7348
OM[3x3]	0.8905	0.8552	0.8051
OM[5x5]	0.888	0.8536	0.8134
OM[7x7]	0.8841	0.8497	0.8122
	QILV	QILV	QILV
WITHOUT FILTER	0.9374	0.8142	0.6451
WIENER	0.7746	0.7567	0.7445
OM[3x3]	0.9331	0.9169	0.8918
OM[5x5]	0.9255	0.9044	0.873
OM[7x7]	0.9181	0.8933	0.8682

Table IV. Woman Blonde

	$\sigma_n = 10$	$\sigma_n = 15$	$\sigma_n = 20$
	PSNR (dB)	PSNR (dB)	PSNR (dB)
WITHOUT FILTER	28.18	24.67	22.18
WIENER	32.04	30.11	28.3
OM[3x3]	32.56	30.55	28.77
OM[5x5]	32.39	30.67	29.17
OM[7x7]	32.24	30.57	29.15
	MSSIM	MSSIM	MSSIM
WITHOUT FILTER	0.648	0.4837	0.3724
WIENER	0.8256	0.759	0.6802
OM[3x3]	0.8491	0.7864	0.7124
OM[5x5]	0.8449	0.7973	0.7428
OM[7x7]	0.8424	0.7974	0.7437
	QILV	QILV	QILV
WITHOUT FILTER	0.8528	0.6293	0.413
WIENER	0.9128	0.9125	0.9042
OM[3x3]	0.9302	0.9105	0.895
OM[5x5]	0.9036	0.8713	0.8389
OM[7x7]	0.8889	0.85	0.81

Table III. Woman Dark-Hair

	$\sigma_n = 10$	$\sigma_n = 15$	$\sigma_n = 20$
	PSNR (dB)	PSNR (dB)	PSNR (dB)
WITHOUT FILTER	28.21	24.68	22.24
WIENER	35.61	32.36	29.84
OM[3x3]	35.51	32.61	30.44
OM[5x5]	36.38	33.65	31.66
OM[7x7]	36.62	34.05	32
	MSSIM	MSSIM	MSSIM
WITHOUT FILTER	0.5276	0.3524	0.2486
WIENER	0.8745	0.7716	0.659
OM[3x3]	0.8676	0.7789	0.69
OM[5x5]	0.8959	0.8261	0.7563
OM[7x7]	0.903	0.8439	0.78
	QILV	QILV	QILV
WITHOUT FILTER	0.3717	0.1378	0.0493
WIENER	0.9671	0.8489	0.6248
OM[3x3]	0.9617	0.8603	0.6995
OM[5x5]	0.9674	0.931	0.852
OM[7x7]	0.9628	0.9314	0.8791

*Fig. 2. Original image Lena*



Fig. 3. Noisy image with Gaussian noise, zero mean and standard deviation $\sigma_n=10$, PSNR (dB)=28.18



Fig. 5. Denoising result with OM 7x7, $T=0.07$, with Gaussian noise, zero mean and standard deviation $\sigma_n =10$, PSNR (dB)=34.42, MSSIM=0.8861, QILV=0.9559



Fig. 4. Denoising result with Wiener, and with Gaussian noise, zero mean and standard deviation $\sigma_n =10$, PSNR (dB)=33.6



Fig. 6. Original image Barbara



Fig. 7. Noisy image with Gaussian noise, zero mean and standard deviation $\sigma_n=10$, PSNR (dB)=28.16



Fig. 9. Denoising result with OM 7x7, $T=0.07$, with Gaussian noise, zero mean and standard deviation $\sigma_n =10$, PSNR (dB)=31.29, MSSIM=0.8841, QILV=0.9181



Fig. 8. Denoising result with Wiener, with Gaussian noise, zero mean and standard deviation $\sigma_n =10$, PSNR (dB)=29.89



Fig. 10. Original image Woman Dark-Hair



Fig. 11. Noisy image with Gaussian noise, zero mean and standard deviation $\sigma_n=10$, PSNR (dB)=28.21



Fig. 13. Denoising result with OM 7x7, $T=0.07$, with Gaussian noise, zero mean and standard deviation $\sigma_n =10$, PSNR (dB)=36.62, MSSIM=0.903, QILV=0.9628



Fig. 12. Denoising result with Wiener, with Gaussian noise, zero mean and standard deviation $\sigma_n =10$, PSNR (dB)=35.61



Fig. 14. Original image Woman Blonde



Fig. 15. Noisy image with Gaussian noise, zero mean and standard deviation $\sigma_n=10$, PSNR (dB)=28.18



Fig. 17. Denoising result with OM 7x7, $T=0.07$, with Gaussian noise, zero mean and standard deviation $\sigma_n=10$, PSNR (dB)=32.28, MSSIM=0.8424, QILV=0.8889



Fig. 16. Denoising result with Wiener, with Gaussian noise, zero mean and standard deviation $\sigma_n=10$, PSNR (dB)=32.04

6. CONCLUSIONS

We have presented a denoising method based on a two-step empirical Bayes approach in the wavelet domain with the characteristic that the estimation of the variance of the coefficients for the “clean” image is performed only at locations corresponding to *father* and *descendant* wavelet coefficients greater than an empirically established threshold T . Compared with the *Wiener* filtering procedure our method (OM) preserves better the high frequency information content in images, see for instance the hair of women, the dress of *Barbara* and tablecloth. Also in uniform regions our method has a good performance, see for instance the cheeks and lips of women. Then our method has a good balance between denoising textured and uniform regions. The results show the correctness of this criterion.

ACKNOWLEDGMENTS

Authors thank the Post-Doctorate Scholarships program, and the PAPIIT IN106816 project from DGAPA in Universidad Nacional Autonoma de Mexico (UNAM) by the support provided during the realization of this research.

REFERENCES

- Aja F., S., San José E., R., Alberola L., C. and Westin, C. F. (2006). "Image quality assessment based on local variance," Proceedings of the 28th IEEE EMBC Annual International Conference, New York, August-September, SaBP2.17, pp. 4815-4818.
- Arivazhagan, S., Sugitha, N. and Vijay, M. (2011). "Adaptive spatial and multiresolution approach for image denoising," in *Proceedings of International Conference on Signal Processing, Communication, Computing and Networking Technologies, ICSCCN*, pp. 812-817.
- Chang, S. G., Yu, B. and Vetterli, M. (2000). "Spatially adaptive wavelet thresholding with context modeling for image denoising," *IEEE Trans. Image Processing*, Vol. 9, No. 9, pp. 1522-1531.
- Jaiswal, A., Upadhyay, J. and Somkuwar, A. (2014). "Image denoising and quality measurements by using filtering and wavelet based techniques," *AUE-International Journal of Electronics and Communications*, Vol. 68, No. 8, pp. 699-705.
- Jaiswal, A. and Upadhyay, J. (2015). "An efficient approach for denoising of noises," *IEEE International Conference on Computer, Communication and Control, IC4*, pp. 1-4.
- Lo Presto, S., Ramchandran, K. and Orchard, M. T. (1997). "Image coding based on mixture modeling of wavelet coefficients and a fast estimation-quantization framework," in *Proc. IEEE Data Compression Conf.*, Snowbird, UT, pp. 221-230.
- Mallat, S. (1989). "A theory for multiresolution signal decomposition: The wavelet representation," *IEEE Trans. on Pattern Anal. Machine Intell.*, Vol. 11, No. 7, pp. 674-693.
- Mihçak, M. K., Kozintsev, I. and Ramchandran, K. (1999). "Spatially adaptive statistical modeling of wavelet image coefficients and its application to denoising," in *Proc. Int. Conf. Acoustics, Speech, and Signal Processing, ICASSP99*, Phoenix, AZ, Vol. 6, March, pp. 3253-3256.
- Mihçak, M. K., Kozintsev, I., Ramchandran, K. and P. Moulin, (1999). "Low-complexity image denoising based on statistical modeling of wavelet coefficients," *IEEE Signal Processing Letters*, Vol. 6, No. 12, pp 300-303.
- Shapiro, J. M. (1993). "Embedded image coding using zerotrees of wavelet coefficients," *IEEE. Trans. on Signal Processing*, Vol. 41, No. 12, pp. 3445-3462.
- Wang, Z., Bovik, A. C., Sheikh, H. R. and Simoncelli, E. P. (2004). "Image quality assessment: From error visibility to structural similarity," *IEEE. Trans. on Image Processing*, Vol. 13, No. 4, pp. 600-612.